Knockdown of arsenic resistance protein 2 inhibits human glioblastoma cell proliferation through the MAPK/ERK pathway

XIAO-XUE KE[1*], YI PANG[1,2*], KUIJUN CHEN[3], DUNKE ZHANG[1], FENG WANG[1], SHUNQIN ZHU[1], JINGXIN MAO[1], XIAOSONG HU[1], GUANGHUI ZHANG[1] and HONGJUAN CUI[1]

[1]Cell Biology Laboratory, State Key Laboratory of Silkworm Genome Biology, Southwest University, Chongqing 400716; [2]Chongqing Engineering Research Center of Antitumor Natural Drugs, Chongqing Three Gorges Medical College, Chongqing 404110; [3]Department 6 of The Research Institute of Surgery, State Key Laboratory of Trauma, Burns and Combined Injury, Daping Hospital, Army Medical University, Chongqing 400042, P.R. China

Received March 28, 2018; Accepted September 27, 2018

DOI: 10.3892/or.2018.6777

Abstract. It is generally known that glioblastoma is the most common primary malignant brain tumor and that it is highly aggressive and deadly. Although surgical and pharmacological therapies have made long-term progress, glioblastoma remains extremely lethal and has an uncommonly low survival rate. Therefore, further elucidation of the molecular mechanisms of glioblastoma initiation and its pathological processes are urgent. Arsenic resistance protein 2 (Ars2) is a highly conserved gene, and it has been found to play an important role in microRNA biosynthesis and cell proliferation in recent years. Furthermore, absence of Ars2 results in developmental death in *Drosophila*, zebrafish and mice. However, there are few studies on the role of Ars2 in regulating tumor development, and the mechanism of its action is mostly unknown. In the present study, we revealed that Ars2 is involved in glioblastoma proliferation and we identified a potential mechanistic role for it in cell cycle control. Our data demonstrated that Ars2 knockdown significantly repressed the proliferation and tumorigenesis abilities of glioblastoma cells *in vitro* and *in vivo*. Further investigation clarified that Ars2 deficiency inhibited the activation of the MAPK/ERK pathway, leading to cell cycle arrest in the G1 phase, resulting in suppression of cell proliferation. These findings support the conclusion that Ars2 is a key regulator of glioblastoma progression.

Correspondence to: Professor Hongjuan Cui, Cell Biology Laboratory, State Key Laboratory of Silkworm Genome Biology, Southwest University, No. 2 Tiansheng Road, BeiBei, Chongqing 400716, P.R. China
E-mail: hongjuan.cui@gmail.com, hcui@swu.edu.cn

*Contributed equally

Key words: Ars2, glioblastoma, cell proliferation, MAPK signaling pathway

Introduction

Glioblastoma (GBM) is the most common primary malignant brain tumor (1), representing 45.2% of malignant tumors and 15.6% of all primary brain tumors. GBM is characterized by rapid proliferation, invasion into the surrounding normal tissue and vascularization, making it highly aggressive and deadly. At present, the standard treatment for newly diagnosed GBM is surgical resection, followed by adjuvant radiotherapy and chemotherapy; however, the prognosis of GBM patients is very poor, with an average survival rate of only 15 months (2) U.S. Therefore, it is urgent and critical to identify alternative therapeutic approaches, and more importantly, to explore the molecular mechanisms underlying GBM initiation and progression.

Arsenic resistance protein 2 (Ars2) is a gene product that was first isolated from a hamster cell line and was found to be resistant to sodium arsenite (2). Ars2 contains several domains: an amino-terminal arginine-rich domain, a central RNA binding domain, and a zinc finger domain, which are all common in RNA-binding proteins (3). Ars2 is a highly conserved gene, which is highly conserved in plants and yeast (4,5). In recent years, many studies have suggested that Ars2 plays an important role in embryonic development (5-7) and in the biosynthesis of microRNAs (8,9); furthermore, it binds to the promoter of Sox2, a positive regulatory transcription factor in neural stem cells (10). The Ars2 gene is necessary for early embryonic development (7,11), and the absence of the Ars2 protein leads to excessive apoptosis in early embryos (5). Ars2 can also be incorporated into the CBP80 and Drosha complexes in the nuclear CBC (12), where it participates in the cutting and maturation of primary miRNAs (13). This incorporation improves the accuracy of the cutting of some miRNAs, including miR-21, let-7 and miR-155 (12). When the expression of Ars2 is downregulated, the processing of pri-miRNA was found to be clearly diminished, and the levels of miRNA were decreased (14-16). In recent years, it has been found that Ars2 is highly expressed in some tumors and that it acts on miR-21 to participate in tumor regulation (17). Some reports have indicated that Ars2 may play a key role in liver cancer and cholangiocarcinoma (17,18). However, there is

little research on Ars2 in tumors, and its mechanism remains unclear. In the present study, we investigated the effects of Ars2 on cell proliferation in glioma growth.

Materials and methods

Cell culture. The human glioblastoma cell lines A172, LN-229, U251 and U87MG, and the human normal brain astrocyte cell line HEB were grown in Dulbecco's modified Eagle's medium (DMEM) supplemented with 10% fetal bovine serum (FBS) plus 1% penicillin and streptomycin (P/S). A172, LN-229 and U87MG cell lines were obtained from the American Type Culture Collection (ATCC; Manassas, VA, USA), U251 was purchased from the China Academia Sinica Cell Repository (Shanghai, China), and HEB was a generous gift from Dr Juan Tan (Southwest Hospital, Army Medical University, Chongqing, China). The identification of cell genetic quality of the cell lines LN-229 and U87MG (HTB-14) was performed using STR profiling by Wuhan Genecreate Biological Engineering Co., Ltd., China. The lentiviral packaging cell line 293FT was cultured in DMEM containing 10% FBS, 0.1 mM MEM non-essential amino acids, 1 mM MEM sodium pyruvate, 4 mM L-glutamine, 1% P/S, and 0.5 mg/ml G418. All cells were cultured at 37˚C in a humidified incubator with 5% CO_2. All the growth media, FBS and supplemental reagents were obtained from Invitrogen/Life Technologies (Thermo Fisher Scientific, Inc., Waltham, MA, USA).

Lentiviral constructs and infection. The lentiviral constructs pLK0.1-puro-GFPsh and pLK0.1-puro-Ars2sh were used in the knockdown studies. First, the lentiviral constructs were transfected into 293FT packaging cells using Invitrogen® Lipofectamine® 2000 reagent (Thermo Fisher Scientific, Inc.). Next, the virus-containing supernatant was harvested and tittered and then used to infect the target cells with 4 μg/ml Polybrene (Santa Cruz Biotechnology, Inc., Dallas, TX, USA). After the final round of infection, the target cells were cultured in the presence of 2 μg/ml puromycin (Life Technologies; Thermo Fisher Scientific, Inc.) for 3 days. Finally, the drug-resistant cells were pooled.

Real-time qPCR assay. Human glioblastoma cells were harvested and lysed with Trizol (Invitrogen®; Thermo Fisher Scientific, Inc.) to purify the total RNA, which was then reverse transcribed into cDNA using M-MLV (Promega Corp., Madison, WI, USA). The mRNA transcript levels of Ars2, NLK, PRKX, GNG12, PAK2, TAOK2, AKT2 and RAC2 were determined by real-time qPCR, using the SYBR® Green PCR Master Mix (Takara). The real-time qPCR assay was performed in triplicate and carried out using the OneStep Plus7500 Real-Time PCR system (Bio-Rad Laboratories, Inc., Hercules, CA, USA) under the following conditions: 95˚C for 10 min, followed by 40 cycles of 5 sec at 95˚C and 30 sec at 60˚C. All of the individual values were normalized to the GAPDH control. Relative mRNA expression levels were calculated by using the ΔΔCq method (19). Sequences of qRT-PCR primers were designed as follows: GAPDH-F: 5'-AACGGATTTGGTCGTATTGGG-3' and GAPDH-R: 5'-CCTGGAAGATGGTGATGGGAT-3'; Ars2-F: 5'-CACCATGTCCTGCCTATCCAG-3' and Ars2-R: 5'-CGAAACCACTCCTCATCTTTGTG-3'; NLK-F: 5'-CGCAAAAATGATGGCGGCTTA-3' and NLK-R: 5'-CCCAGGGTTTAACATGGCTG-3'; PRKX-F: 5'-CTGGACGTGGCATGACGAG-3' and PRKX-R: 5'-TCGATGGCACAGATGATCTCT-3'; GNG12-F: 5'-AGCAAGCACCAACAATATAGCC-3' and GNG12-R: 5'-AGTAGGACATGAGGTCCGCT-3'; PAK2-F: 5'-CACCCGCAGTAGTGACAGAG-3' and PAK2-R: 5'-GGGTCAATTACAGACCGTGTG-3'; TAOK2-F: 5'-GGACTTTGGTTCTGCGTCCAT-3' and TAOK2-R: 5'-TCGATGCAGGTTATCCCCAAG-3'; AKT2-F: 5'-GGTGCAGAGATTGTCTCGGC-3' and AKT2-R: 5'-GCCCGGCCATAGTCATTGTC-3'; RAC2-F: 5'-TCTGCTTCTCCCTCGTCAG-3' and RAC2-R: 5'-TCACCGAGTCAATCTCCTTGG-3'.

Western blotting. Human glioblastoma cells or xenograft tumors were harvested and washed once with ice-cold PBS. Cell pellets or tumor tissues were suspended in SDS sample buffer, boiled for 10 min and then centrifuged at 10,000 x g for 10 min. Fifty micrograms of the protein samples were separated using 10% SDS-polyacrylamide gel electrophoresis (SDS-PAGE) and transferred to a PVDF membrane (EMD Millipore Corp., Billerica, MA, USA). Next, the PVDF membrane was probed with both primary and secondary antibodies and finally visualized by enhanced chemiluminescence (ECL) (Beyotime Institute of Biotechnology, Haimen, China). The primary antibodies were as follows: Rabbit anti-human Ars2 (dilution 1:2,000; cat. no. ab192999; Abcam, Cambridge, UK), mouse anti-human α-tubulin (dilution 1:2,000; cat. no. B-5-1-2; Sigma-Aldrich; Merck KGaA, Darmstadt, Germany), rabbit anti-human CDK2 (dilution 1:1,000; cat. no. 2546S; Cell Signaling Technology, Inc., Danvers, MA, USA), rabbit anti-human CDK4 (dilution 1:1,000; cat. no. 12790S; Cell Signaling Technology), rabbit anti-human cyclin D1 (dilution 1:1,000; cat. no. 2922S; Cell Signaling Technology), rabbit anti-human cyclin E2 (dilution 1:1,000; cat. no. ab40890; Abcam), rabbit anti-human p21 (dilution 1:1,000; cat. no. ab109199; Abcam), rabbit anti-human PAK2 (dilution 1:1,000; cat. no. 2608S; Cell Signaling Technology), rabbit anti-human ERK1/2 (dilution 1:500; cat. no. 4695S; Cell Signaling Technology), rabbit anti-human phospho-ERK1/2 (Thr202/Tyr204) (dilution 1:2,000; cat. no. 4376S; Cell Signaling Technology), rabbit anti-human MEK1/2 (dilution 1:1,000; cat. no. 9122S; Cell Signaling Technology), and rabbit anti-human phospho-MEK1/2 (Ser217/221) (1:500; cat. no. 9121S; Cell Signaling Technology). Horseradish peroxidase-conjugated goat anti-mouse and goat anti-rabbit IgG (1:20,000; KPL, Inc., Gaithersburg, MD, USA) were used as secondary antibodies.

Histology and immunohistochemistry. The tumor tissue was embedded in paraffin blocks, sectioned at a thickness of 4 μm and stained with hematoxylin and eosin (H&E). For the immunohistochemical examination, the sections were deparaffinized, rehydrated, and then treated with 10 mmol/l citrate buffer (pH 6.0) at 95˚C for antigen retrieval, and subsequently washed in PBS. The endogenous peroxidase activity was quenched with 0.6% H_2O_2 in methanol, and the sections were blocked with normal goat serum. They were

then incubated sequentially with primary antibodies, rabbit anti-human Ars2 (dilution 1:100; cat. no. NBP2-15473; Novus Biologicals, Littleton, CO, USA), mouse anti-Ki-67 (dilution 1:100; clone no. 550609; BD Pharmingen; BD Biosciences, San Jose CA, USA), and secondary antibodies, biotinylated goat anti-rabbit, goat anti-mouse IgG, and the ABC reagent (Vector Laboratories, Inc., Burlingame, CA, USA). The immunostaining was visualized with 3,3'-diaminobenzidine (Sigma-Aldrich; Merck KGaA). The sections were then counterstained with hematoxylin before being examined using a Nikon 80i light microscope (Nikon, Tokyo, Japan). Nuclear immunostaining was considered as positive for protein accumulation. The immunohistochemistry staining score was identified as 0 (no detectable immunostaining), 1 (few nuclei), 2 (up to 10% of nuclei), 3 (10-50% nuclei), and 4 (>50% nuclei) (20-22).

Cell growth and proliferation assays. U87MG and LN-229 cells were seeded and cultured in 6-well culture plates at a concentration of $1x10^5$ cells/well. For the cell growth assays, the cells were harvested and counted daily for 7 days using a hemocytometer, and cell growth was monitored using trypan blue dye analysis. For the cell proliferation assays, U87MG and LN-229 cells were plated in 96-well culture plates. The cell proliferation was determined by MTT (Sigma-Aldrich; Merck KGaA) analysis. Briefly, 10 μl of MTT was added into 100 μl of medium in each well, and the cells were incubated at 37˚C for 2 h. Next, 100 μl of DMSO was added to each well to dissolve MTT, and the plate was shaken for 20 min on the table concentrator. The absorbance was measured at a wavelength of 560 nm using a microplate reader (Model 550; Bio-Rad Laboratories).

BrdU staining. U87MG and LN-229 cells were seeded and cultured in 24-well culture plates at a concentration of $2x10^3$ cells/well. The cells were then incubated with 10 μg/ml BrdU (Sigma-Aldrich; Merck KGaA) for 1 h, washed with phosphate-buffered saline (PBS), and fixed in 4% paraformaldehyde (PFA) for 20 min. Subsequently, the cells were pretreated with 1 mol/l HCl and blocked with 10% goat serum for 1 h, followed by staining with a monoclonal rat primary antibody against BrdU (dilution 1:200; cat. no. ab6326; Abcam) at 4˚C overnight. They were then incubated with the Alexa FluorR® 594 goat anti-rat IgG secondary antibody (H+L; Invitrogen; Thermo Fisher Scientific, Inc.) for 2 h. DAPI (300 nM) was used for nuclear staining, and the percentage of BrdU-positive cells was calculated from at least 10 microscopic fields (Olympus CKX41; Olympus Corp., Tokyo, Japan).

Soft agar clonogenic assay. U87MG cells were mixed in 0.3% Noble agar in DMEM supplemented with 10% FBS and plated at 1,500 cells/well into 6-well plates containing a solidified bottom layer (0.6% Noble agar in the same growth medium). After 21 days, colonies were stained with 5 mg/ml MTT and photographed using an Olympus CKX41 inverted miscroscope (Olympus Corp.).

Tumor xenograft assay. Six female NOD/SCID mice (4 weeks of age, 18 g of average weight) were used in the xenograft assay, and they were maintained under specific pathogen-free (SPF) conditions in the animal facility of Southwest University (Chongqing, China). In generally, all mice were housed in the SPF room with temperature 20-26˚C, and the air cleanliness was ten thousand grade (≥0.5 μm particles ≤ ten thousand/cubic foot). The animal illumination and working illumination were controlled in 15-20 Lx and 150-300 Lx respectively, and the alternation time of light and shade was 12/12 h. The SPF mice fodder was purchased from Chongqing TengXin Biotechnology Co., Ltd. (Chongqing, China). The drinking water of mice was sterilized by high pressure steam (121.3˚C, 25 min) before use. For each mouse, both flanks were injected subcutaneously with $1x10^6$ U87MG cells suspended in 200 μl of serum-free DMEM. One week after tumor cell injection, tumor growth was measured using calipers, and tumor volume was calculated using the formula $4/3\pi r^3$, where 'r' is the radius of the tumor. The xenograft tumors were removed and weighed after three weeks of growth. The tumors were washed with ice-cold PBS and prepared for the following histological, immunohistochemical and western blot assays.

Flow cytometry. For cell cycle analysis, $1x10^6$ cells were harvested and washed twice with ice-cold PBS, fixed with 70% ethanol, stained with propidium iodide (PI) (BD Biosciences), and incubated with RNaseA for 30 min at room temperature. For the cell apoptosis analysis, adherent and floating cells were pooled, collected by centrifugation at 211 x g for 5 min, and washed once with ice-cold PBS. Apoptotic cells were determined using the Annexin V-fluorescein isothiocyanate (FITC) kit (Sigma-Aldrich; Merck KGaA) according to the manufacturer's instructions. Finally, the samples were analyzed by flow cytometry using a FACS C6 (BD Biosciences), and the data were analyzed with BD CellQuest Pro software (BD Biosciences).

Inhibitor treatment. The MEK inhibitor, trametinib, was purchased from MCE® MedChemExpress (Monmouth Junction, NJ, USA). The vector encoding human Ars2 was constructed by PCR-based amplification and subsequently cloned into the pCDH-CMV-MCS-EF1-copGFP vector to generate the recombinant plasmid. U87MG cells were prepared to 70-80% confluence in 6-well plates, and were transiently transfected with plasmids using Invitrogen® Lipofectamine® 2000 reagent (Thermo Fisher Scientific, Inc.). At 48 h after transfection, U87MG cells were harvested and plated in 96-well culture plates. Then cells were treated with 2 nM (23,24) trametinib, and the cell proliferation was determined by MTT assay.

Patient tumor tissues. All patient tissues used in the experiment were purchased as a tissue microarray from Alenabio Company (Item no: BS17015a, BS17016a; http://www.alenabio.com). The brain tumor microarray chip BS17015a included 38 cases of astrocytoma, 14 cases of glioblastoma, 6 cases of oligodendrocytoma, 1 case of anaplastic ependymoma, 1 case of medulloblastoma, and 3 cases of peripheral brain tissue, one point of each sample. And the glioma tissue microarray chip BS17016a included 35 cases of glioma with different pathological stage and 5 cases of normal peripheral tissue, taking two points for each sample.

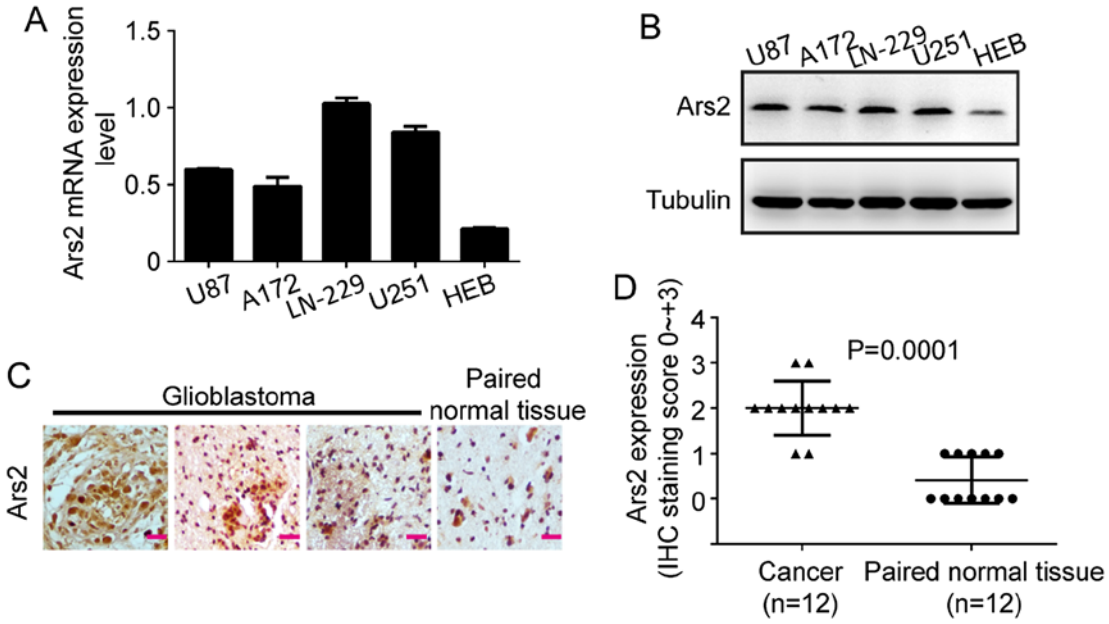

Figure 1. Ars2 is commonly expressed in glioblastoma cells. (A) Real-time qPCR analysis of Ars2 mRNA expression levels in four glioblastoma cell lines (U87, A172, LN-229 and U251) and one normal astrocyte cell line (HEB). The data represent the average obtained from three independent experiments and are presented as the mean ± SD. (B) Western blot analysis of Ars2 expression in four glioblastoma cell lines and one normal astrocyte cell line. α-tubulin is shown as the loading control. (C) Immunohistochemical analysis of Ars2 expression in human glioblastoma tumor and paired normal tissues. Scale bar, 10 μm. (D) Statistical analyses of immunohistochemical results of Ars2 expression levels in 12 paired samples of normal and glioblastoma tissues; P=0.0001. Ars2, arsenic resistance protein 2.

Quantification and statistical analysis. Each value was confirmed using at least three independent experiments. Quantitative data are expressed as the mean ± SD. GraphPad Prism 6 (GraphPad Software, Inc., La Jolla, CA, USA) was applied for statistical analysis. A two-tailed Student's t-test was performed for paired samples. One- or two-way analysis of variance, followed by Dunnett's or Bonferroni's multiple comparison were performed for comparing multiple groups. $P<0.05$ was considered to indicate a statistically significant result. All calculations were performed using the SPSS software package 14.0 (SPSS, Inc., Chicago, IL, USA).

Results

Ars2 is commonly expressed in glioblastoma. To investigate whether Ars2 is associated with glioblastoma cell proliferation, we first examined the expression levels of Ars2 in various human glioblastoma cell lines and tumor tissues. The results of qRT-PCR and western blot analyses showed that Ars2 was commonly expressed in four glioblastoma cell lines (Fig. 1A and B), such as A172, LN-229, U87MG and U251. In addition, the results revealed that Ars2 was expressed at a higher level in tumor cells than that in HEB, a normal human brain astrocyte cell line. The results of the immunohistochemical assay in 12 paired samples showed that Ars2 was highly expressed in human glioblastoma tissues and was lower in adjacent normal brain tissues (Fig. 1C and D). Therefore, we proposed that Ars2 may have an important role in glioblastoma.

Knockdown of Ars2 inhibits the proliferation and self-renewal of glioblastoma cells. To confirm the connection between Ars2 and glioblastoma cell proliferation, we performed downregulation analysis of Ars2 in glioblastoma cells. We knocked down Ars2 in LN-229 and U87MG cells, with GFPsh as a control (Fig. 2A). The results of the cell counting and MTT analyses verified that downregulation of Ars2 significantly inhibited the proliferation of LN-229 and U87MG cells (Fig. 2B and C). Moreover, we performed BrdU staining to confirm the cell proliferation status (25), and the results showed that the percentage of BrdU-positive cells was significantly decreased after Ars2 knockdown (Fig. 3A and B). Next, we checked for a functional role of Ars2 in maintaining the self-renewal ability of U87MG cells. The results showed that U87MG-Ars2-knockdown cells gave rise to tiny and scant colonies in soft agar, and these cells formed small spheres, when compared to the control (Fig. 3C and D). These data revealed that downregulation of Ars2 significantly inhibited the proliferation and self-renewal ability of glioblastoma cells, indicating that the Ars2 gene may be a key factor in glioblastoma growth.

Knockdown of Ars2 inhibits tumorigenicity of glioblastoma cells. Next, the xenograft tumor growth assay was performed to test for a role of Ars2 in the regulation of the tumorigenicity of glioblastoma cells. U87MG-Ars2sh cells were injected into NOD/SCID mice to form xenograft tumors, and U87MG-GFPsh cells were used as control. As shown in Fig. 4A, the volume of the xenograft tumors in the Ars2sh group was much lower than that calculated in the GFPsh group, indicating that downregulation of Ars2 inhibited the tumorigenicity of neuroblastoma cells. Furthermore, the tumor weights of the Ars2sh group were much lower than in the GFPsh group (Fig. 4B). Furthermore, to investigate the cell proliferation

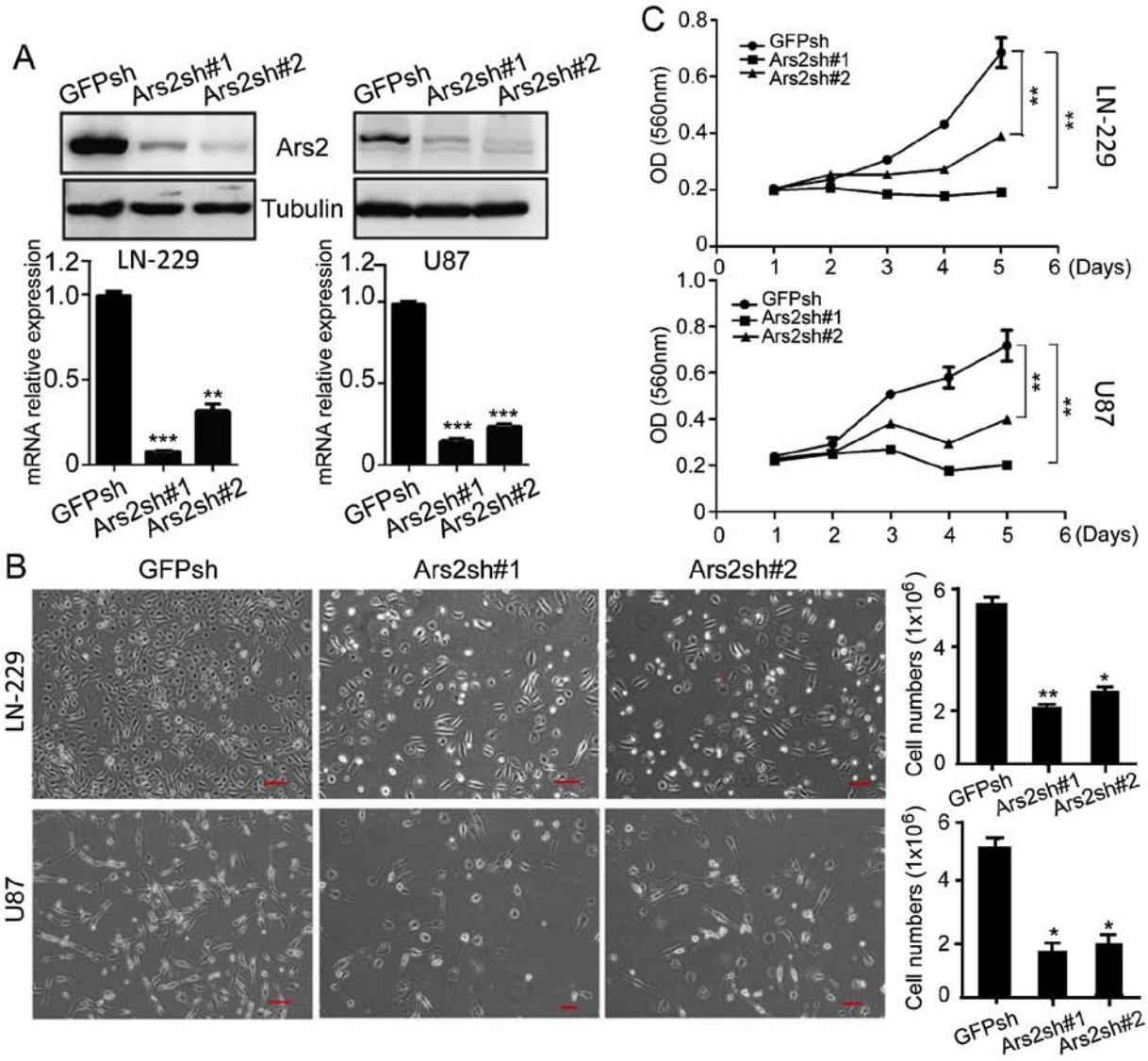

Figure 2. Downregulation of Ars2 inhibits glioblastoma cell proliferation. (A) Top panels: Western blot analysis of Ars2 expression in glioblastoma cells with GFP knockdown or Ars2 knockdown; α-tubulin is shown as the loading control. Lower panels: Real-time qPCR analysis of Ars2 mRNA expression levels in glioblastoma cells with GFP knockdown or Ars2 knockdown. (B) Left panels: Morphologic examination of glioblastoma cells with GFP knockdown or Ars2 knockdown. Right panels: Cell counting analysis with trypan blue dye staining. (C) Cell growth curves of glioblastoma cells with GFP knockdown or Ars2 knockdown were analyzed by MTT assay. For all data in A-C, each value represents the average obtained from three independent experiments, and the data are presented as the mean ± SD (error bars). Statistical analyses were performed using two-tailed Student's t-tests, $^{***}P<0.001$, $^{**}P<0.01$, $^{*}P<0.05$. Ars2, arsenic resistance protein 2.

status of the xenograft tumors, the tumors were removed and then checked by immunoblot and immunohistochemical analyses. The results shown in Fig. 4C and D demonstrated that downregulation of Ars2 significantly decreased the number of Ki67-positive cells, indicating that the cell proliferation in xenograft tumors was inhibited by Ars2 knockdown. All of the above data indicated that Ars2 knockdown inhibited the tumorigenicity of glioblastoma cells.

Ars2 is involved in MAPK pathway activation and is associated with the glioblastoma cell cycle. Since Ars2 knockdown inhibits the proliferation and tumorigenicity of glioblastoma cells, we used flow cytometric detection to test how Ars2 influences glioblastoma cell proliferation. As shown in Fig. 5A, downregulation of Ars2 in glioblastoma cells induced cell cycle arrest in the G1 phase; furthermore, the number of S phase cells was clearly decreased after Ars2 knockdown. We next analyzed the expression of cell cycle-related proteins. The result of the western blot analysis verified that downregulation of Ars2 significantly decreased the expression of CDK2 and cyclin E2 (Fig. 5B), which are required for the transition from G1 to S phase in the cell cycle. There was also a marked upregulation of P21 expression (Fig. 5B). This protein is known as cyclin-dependent kinase inhibitor 1 and is primarily associated with inhibition of CDK2 (26-28). These results confirmed that knockdown of Ars2 inhibited cell cycle progression.

In addition, we assessed cell apoptosis after knockdown of Ars2. As shown in Fig. 5C, the result revealed that there was no significant difference between the Ars2 knockdown group and the control group. However, we found that the MAPK/ERK pathway was inhibited after Ars2 knockdown

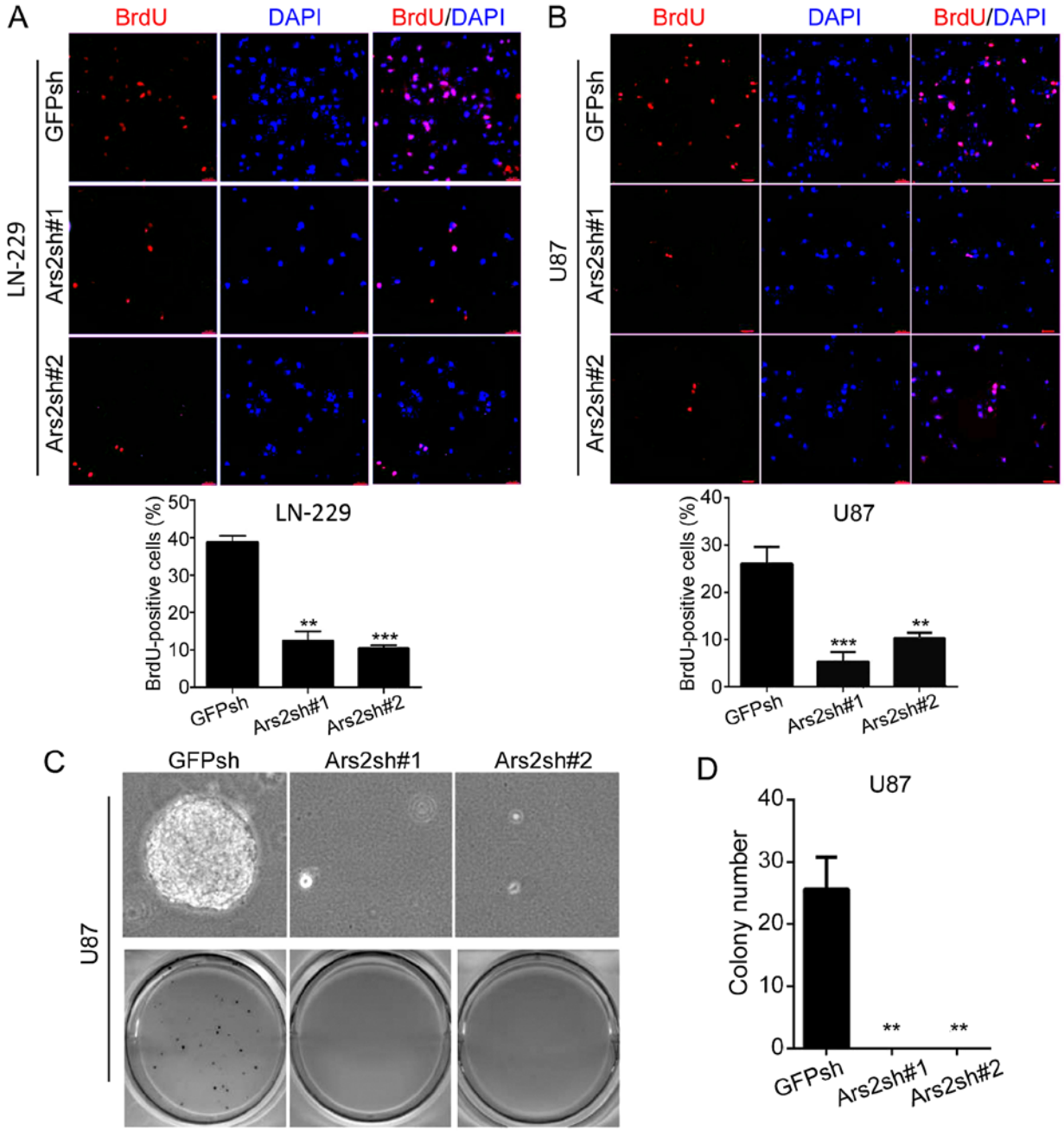

Figure 3. Downregulation of Ars2 inhibits BrdU incorporation and the self-renewal ability of glioblastoma cells. (A and B) Glioblastoma cells with GFP knockdown or Ars2 knockdown were plated at $2x10^3$ cells per well in 24-well culture plates. After cells were adherent, a 1-h incubation with BrdU was performed, and the immunofluorescence was detected by anti-BrdU antibody. Scale bar, 20 μm. Finally, the ratio of BrdU-positive cells was calculated. (C) U87MG cells with GFP knockdown or Ars2 knockdown were plated at $1x10^3$ cells per well in 6-well culture plates. After 14 to 21 days of culture, soft agar colonies grew from cells with GFP knockdown or Ars2 knockdown. As shown, cells with Ars2 knockdown were observed to give rise to tiny and scant colonies in soft agar. Colonies >0.5 mm or those containing >50 cells were recorded. For all the data in A, B and D, each value represents the average obtained from three independent experiments and the error bars show the SD. Statistical analyses were performed using two-tailed Student's t-tests, $^{***}P<0.001$, $^{**}P<0.01$. Ars2, arsenic resistance protein 2.

(Fig. 5D). It is known that activation of the MAPK/ERK pathway is necessary and sufficient to promote production of the cyclin E/CDK2 complex, which allows progression from G1-phase to S-phase in most mammalian cells (29-31). The results in Fig. 5D show that the phosphorylation and activation of MEK and ERK were both inhibited by Ars2 knockdown. To further confirm that the effect of Ars2 knockdown on cell proliferation was dependent on the MAPK/ERK pathway, we next overexpressed Ars2 in MAPK inhibitor-treated U87MG cells. Overexpression of Ars2 restored cell proliferation in the MAPK inhibitor-treated cells (Fig. 5E), suggesting that the reduced cell proliferation induced by knockdown of Ars2 is due to the inhibition of the MAPK/ERK pathway. Our findings provide new insight into the mechanism of how Ars2 regulates cell cycle entry and cell proliferation by showing that Ars2 knockdown leads to inhibition of the MAPK/ERK pathway, ultimately resulting in the suppression of cell cycle progression and cell proliferation.

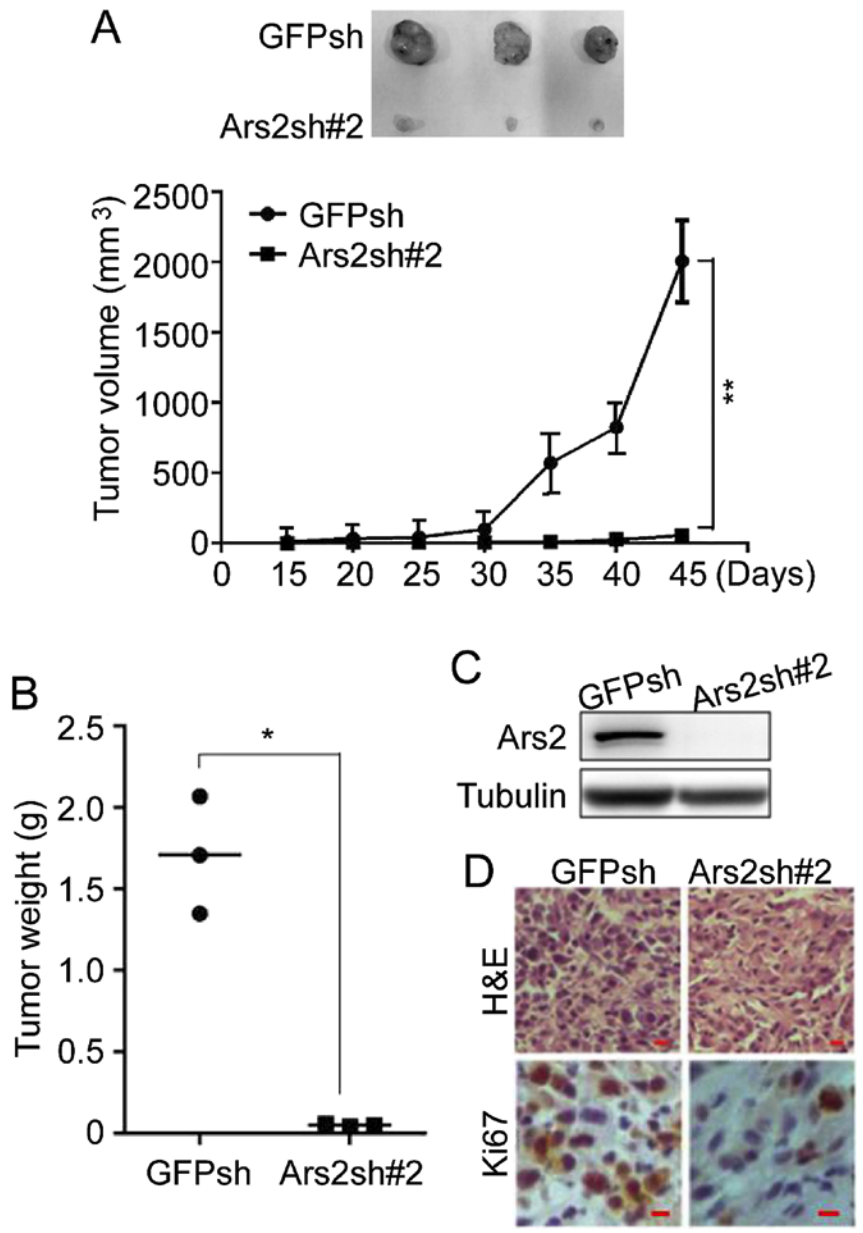

Figure 4. Downregulation of Ars2 inhibits the tumorigenicity of glioblastoma cells. (A) Tumor growth in NOD/SCID mice inoculated with the indicated U87MG cells, and measurement of xenograft tumor volume using calipers. (B) Xenograft tumor weight was measured after the tumors were removed. For all of the data in A and B, each value represents the average obtained from three independent experiments and the error bars show the SD. Statistical analyses were performed using two-tailed Student's t-tests, $^{**}P<0.01$, $^{*}P<0.05$. (C) Western blot analysis of Ars2 expression in xenograft tumors formed by the indicated U87MG cells. α-tubulin is shown as the loading control. (D) Histological analysis of xenograft tumor tissue and immunohistochemical analysis of Ki67 expression in xenograft tumors derived from the indicated U87MG cells. Ars2, arsenic resistance protein 2.

Discussion

Ars2 is a highly conservative gene located on the long arm of human chromosome 7 (32). It is reported that Ars2 plays an important role in the biosynthesis of microRNAs, and loss of Ars2 leads to decreased levels of a variety of microRNAs, including miR-21, miR-155 and let-7 (12,13). Some researchers have observed that the expression of Ars2 in cholangiocarcinoma tissues is significantly higher than that in paracancerous tissues (18), and that the expression of Ars2 is positively correlated to the expression of miR-21, but negatively correlated with the expression of PTEN and PDCD4 (17). After interfering with Ars2 function, the proliferation and invasion of cholangiocarcinoma cells were weakened, and the formation of mature miR-21 molecules was inhibited (17). However, the role of Ars2 in glioblastoma and its molecular mechanism have not yet been reported. Our present results provide evidence that Ars2 regulates glioblastoma proliferation and the cell cycle.

The basic process of cellular life is the cell cycle, and infinite progression through the cell cycle allows cells to proliferate. In the course of continuous evolution, cells establish a series of regulatory mechanisms to ensure that the cell cycle proceeds in an orderly manner to allow cells to maintain normal tissue structure and function (33). When the proliferation of cells is not controlled by the body and there is infinite proliferation,

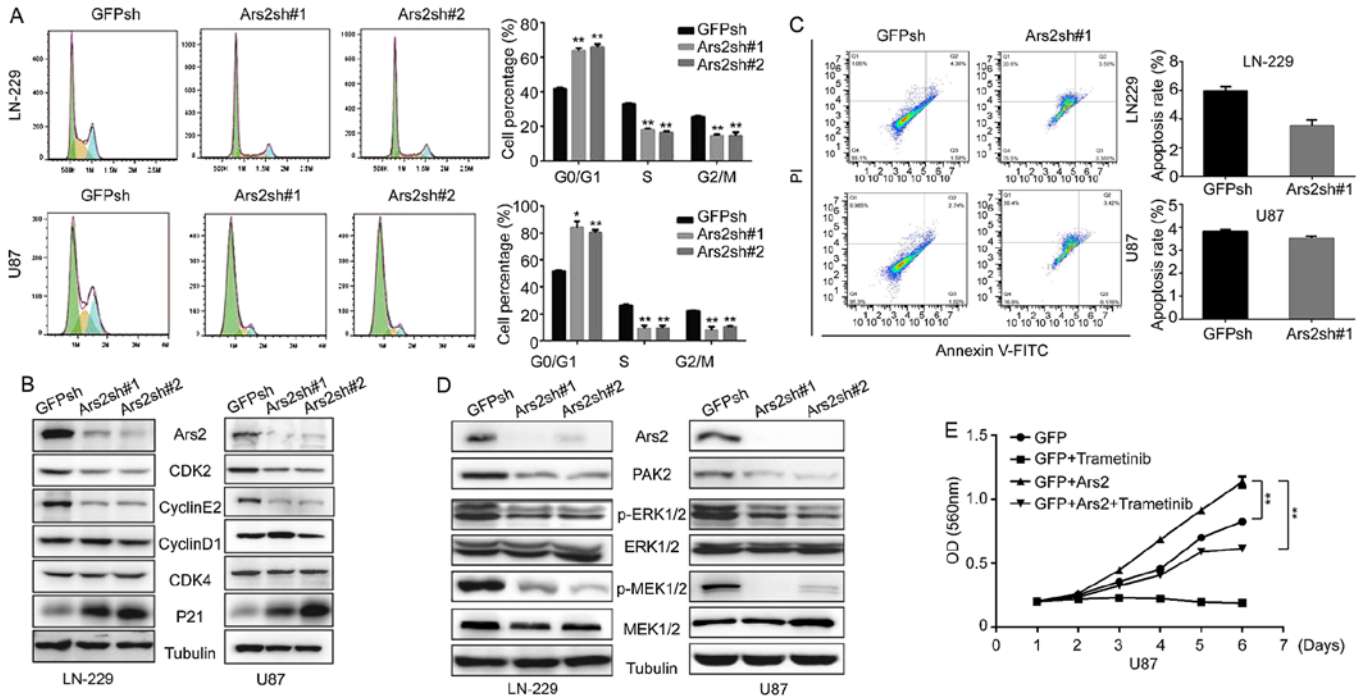

Figure 5. Downregulation of Ars2 inhibits the cell cycle and the MAPK/ERK pathway in glioblastoma cells. (A) Cell cycle distribution of the indicated glioblastoma cells was determined by flow cytometry and then statistical analysis was performed to clarify the cell cycle phase percentage. Each value represents the average obtained from three independent experiments and the error bars show the SD. Statistical analyses were performed using two-tailed Student's t-tests, $^{**}P<0.01$, $^{*}P<0.05$. (B) Western blot analysis of the expression of cell cycle-regulating cyclins and CDKs in glioblastoma cells with Ars2 knockdown. α-tubulin is shown as the loading control. (C) Cell apoptosis of the indicated glioblastoma cells was determined by flow cytometry and then statistical analysis was performed to clarify cell apoptosis percentage. Each value represents the average obtained from three independent experiments and the error bars show the SD. Statistical analyses were performed using two-tailed Student's t-tests, and there was no significant statistical difference. (D) Western blot analysis of the expression of proteins in the MAPK/ERK pathway in glioblastoma cells with Ars2 knockdown. α-tubulin is shown as the loading control. (E) Cell growth curves of MAPK inhibitor-treated U87MG cells with GFP overexpression or Ars2 overexpression were analyzed by MTT assay. Trametinib, a potent MEK inhibitor that specifically inhibits MEK1/2. Each value represents the average obtained from three independent experiments, and the data are presented as the mean ± SD (error bars). Statistical analyses were performed using two-tailed Student's t-tests, $^{**}P<0.01$. Ars2, arsenic resistance protein 2.

cancer is formed (34). The cell cycle is regulated by the activities of cyclin-CDK complexes (35), and abnormalities of cyclin and CDKs, or the absence of CDK inhibitors, can cause cell cycle disorders, leading to out-of-control cell proliferation (34). In response to extracellular signals, such as growth factors, cyclin D is the first cyclin produced in the cell cycle and it binds to existing CDK4 to form the active cyclin D-CDK4 complex (36,37). The cyclin D-CDK4 complex in turn phosphorylates the retinoblastoma susceptibility protein (Rb), and the hyperphosphorylated Rb separates from the E2F/DP1/Rb complex to activate E2F (38). Activation of E2F results in transcriptional activation of certain key factors such as cyclin E, cyclin A, DNA polymerase, among others (36). Cyclin E binds to CDK2, forming the cyclin E-CDK2 complex, which pushes the cell from the G1 to S phase (39). In the present study, our findings showed that Ars2 knockdown dramatically suppressed expression of cyclin E and CDK2, and upregulated P21 expression. This may be the major reason that caused the cell cycle arrest in the G1 phase, which then induced the inhibition of cell proliferation and tumorigenicity of glioblastoma cells.

In the last few decades, a number of studies have illustrated that the most basic feature of cancer cells is that they can maintain unlimited proliferation. It was found that 40% of human melanomas contain activating mutations that can affect the structure of the B-Raf protein, consequently affecting the basic signaling function of the Raf mitogen-activated protein kinase (MAPK) pathway, thus affecting cell proliferation (40). It is known that the MAPK/ERK pathway plays an important role in promoting cell growth and proliferation in many mammalian cells (31). In general, the presence of extracellular growth signals trigger the activation of canonical receptor tyrosine kinases and subsequent activation of the small GTPase Ras (31), which then leads to a series of phosphorylation events downstream in the MAPK cascade (Raf-MEK-ERK), ultimately resulting in the phosphorylation and activation of MAPK/ERK. The activation of MAPK/ERK kinase activity causes the phosphorylation of its many downstream targets, including the cyclin D-CDK4 complex (4), which contributes to the hyperphosphorylation of Rb and the subsequent activation of E2F (40), promoting the expression of its targets cyclin E and CDK2, finally allowing cells to progress from G1 to S-phase (4,31,40). Thus, we investigated the MAPK/ERK pathway in our study. We found that the MAPK/ERK pathway is crucial for the regulation of glioblastoma cell proliferation by Ars2. The activation and phosphorylation of MEK and ERK were both inhibited by Ars2 knockdown. Moreover, overexpression of Ars2 restored cell proliferation of glioblastoma cells treated by the MAPK inhibitor. Our results provide evidence of the regulation of cell proliferation by Ars2 through the MAPK/ERK pathway.

In summary, in our research, we verified an important role of Ars2 in glioblastoma cell proliferation and tumorigenicity. Our results confirmed that Ars2 knockdown led to the

suppression of proliferation, self-renewal and tumorigenicity of glioblastoma cells. Additionally, Ars2 knockdown induced the downregulation of MEK1/2 and ERK1/2 phosphorylation, leading to inhibition of the MAPK/ERK pathway. This effect then led to decreased cyclin E2 and CDK2 expression, finally causing G1 arrest in the glioblastoma cells that ultimately repressed cell proliferation. In accordance with these results, we confirmed that Ars2 serves as an important mediator in regulating glioblastoma cell proliferation and maintaining stemness, and we suggest that Ars2 may be a potential therapeutic target for glioblastoma treatment. Moreover, Ars2 was reported to play important roles in microRNA biosynthesis (8,9,12), and consequently many microRNAs were found to affect cancer development in recent years (41-44). It should be important to ascertain the association among Ars2, microRNAs and cancer. Therefore, we will focus on the regulatory mechanism of Ars2 linked with microRNAs in cancer, and explore the potential correlation of Ars2, microRNAs, the MAPK pathway and cancer cell proliferation in future research.

Acknowledgements

Not applicable.

Funding

The present study was supported by the National Natural Science Foundation of China (grant nos. 81502574, 31501100 and 81672502), the Chongqing Research Program of Basic Research and Frontier Technology (grant no. cstc2017jcyjAX0304), the Fundamental Research Funds for the Central Universities (grant no. SWU118033), the Chongqing University Innovation Team Building Special Fund (grant no. CXTDX201601010), and the Natural Science Research Projects of Chongqing Three Gorges Medical College (grant no. 2016xmpxz04).

Availability of data and materials

The datasets used during the present study are available from the corresponding author upon reasonable request.

Authors' contributions

XXK and YP carried out the most of the experiments. XXK wrote the paper, and YP helped to edit the manuscript. KC, DZ and FW participated in the cell experiments and animal experiments. SZ and JM helped to do statistical analysis and the flow cytometry analysis. XH and GZ participated in immunoblot assays and immunofluorescence staining. HC conceived, designed the study and helped to revise the manuscript. All authors read and approved the manuscript and agree to be accountable for all aspects of the research in ensuring that the accuracy or integrity of any part of the work are appropriately investigated and resolved.

Ethics approval and consent to participate

This study was conducted in accordance with approved guidelines. The animal study protocol was preapproved by the Institutional Animal Care and Use Committee of Southwest University. All efforts were made to minimize animal suffering. The patient tissue microarray used in the experiment was obtained from Alenabio Company. All the patients provided written informed consent to participate. Tissue analysis was also approved by the Ethics Committee of the Southwest University.

Patient consent for publication

Not applicable.

Competing interests

The authors disclose no potential conflicts of interest.

References

1. Ostrom QT, Gittleman H, Farah P, Ondracek A, Chen Y, Wolinsky Y, Stroup NE, Kruchko C and Barnholtz-Sloan JS: CBTRUS statistical report: Primary brain and central nervous system tumors diagnosed in the United States in 2006-2010. Neuro Oncol 15 (Suppl 2): ii1-56, 2013.
2. Rossman TG and Wang Z: Expression cloning for arsenite-resistance resulted in isolation of tumor-suppressor fau cDNA: Possible involvement of the ubiquitin system in arsenic carcinogenesis. Carcinogenesis 20: 311-316, 1999.
3. Gruber JJ, Olejniczak SH, Yong J, La Rocca G, Dreyfuss G and Thompson CB: Ars2 promotes proper replication-dependent histone mRNA 3' end formation. Mol Cell 45: 87-98, 2012.
4. Wilson MD, Riemer C, Martindale DW, Schnupf P, Boright AP, Cheung TL, Hardy DM, Schwartz S, Scherer SW, Tsui LC, *et al*: Comparative analysis of the gene-dense ACHE/TFR2 region on human chromosome 7q22 with the orthologous region on mouse chromosome 5. Nucleic Acids Res 29: 1352-1365, 2001.
5. Wilson MD, Wang D, Wagner R, Breyssens H, Gertsenstein M, Lobe C, Lu X, Nagy A, Burke RD, Koop BF and Howard PL: ARS2 is a conserved eukaryotic gene essential for early mammalian development. Mol Cell Biol 28: 1503-1514, 2008.
6. Prigge MJ and Wagner DR: The arabidopsis serrate gene encodes a zinc-finger protein required for normal shoot development. Plant Cell 13: 1263-1279, 2001.
7. Amsterdam A, Nissen RM, Sun Z, Swindell EC, Farrington S and Hopkins N: Identification of 315 genes essential for early zebrafish development. Proc Natl Acad Sci USA 101: 12792-12797, 2004.
8. Grigg SP, Canales C, Hay A and Tsiantis M: SERRATE coordinates shoot meristem function and leaf axial patterning in Arabidopsis. Nature 437: 1022-1026, 2005.
9. Yang L, Liu Z, Lu F, Dong A and Huang H: SERRATE is a novel nuclear regulator in primary microRNA processing in Arabidopsis. Plant J 47: 841-850, 2006.
10. Andreu-Agullo C, Maurin T, Thompson CB and Lai EC: Ars2 maintains neural stem-cell identity through direct transcriptional activation of Sox2. Nature 481: 195-198, 2011.
11. Golling G, Amsterdam A, Sun Z, Antonelli M, Maldonado E, Chen W, Burgess S, Haldi M, Artzt K, Farrington S, *et al*: Insertional mutagenesis in zebrafish rapidly identifies genes essential for early vertebrate development. Nat Genet 31: 135-140, 2002.
12. Sabin LR, Zhou R, Gruber JJ, Lukinova N, Bambina S, Berman A, Lau CK, Thompson CB and Cherry S: Ars2 regulates both miRNA- and siRNA- dependent silencing and suppresses RNA virus infection in Drosophila. Cell 138: 340-351, 2009.
13. Gruber JJ, Zatechka DS, Sabin LR, Yong J, Lum JJ, Kong M, Zong WX, Zhang Z, Lau CK, Rawlings J, *et al*: Ars2 links the nuclear cap-binding complex to RNA interference and cell proliferation. Cell 138: 328-339, 2009.
14. Denli AM, Tops BB, Plasterk RH, Ketting RF and Hannon GJ: Processing of primary microRNAs by the Microprocessor complex. Nature 432: 231-235, 2004.
15. Han J, Lee Y, Yeom KH, Kim YK, Jin H and Kim VN: The Drosha-DGCR8 complex in primary microRNA processing. Genes Dev 18: 3016-3027, 2004.

16. Landthaler M, Yalcin A and Tuschl T: The human DiGeorge syndrome critical region gene 8 and Its D. Melanogaster homolog are required for miRNA biogenesis. Curr Biol 14: 2162-2167, 2004.
17. He Q, Cai L, Shuai L, Li D, Wang C, Liu Y, Li X, Li Z and Wang S: Ars2 is overexpressed in human cholangiocarcinomas and its depletion increases PTEN and PDCD4 by decreasing microRNA-21. Mol Carcinog 52: 286-296, 2013.
18. He Q, Huang Y, Cai L, Zhang S and Zhang C: Expression and prognostic value of Ars2 in hepatocellular carcinoma. Int J Clin Oncol 19: 880-888, 2014.
19. Livak KJ and Schmittgen TD: Analysis of relative gene expression data using real-time quantitative PCR and the 2(-Delta Delta C(T)) method. Methods 25: 402-408, 2001.
20. Charafe-Jauffret E, Tarpin C, Bardou VJ, Bertucci F, Ginestier C, Braud AC, Puig B, Geneix J, Hassoun J, Birnbaum D, *et al*: Immunophenotypic analysis of inflammatory breast cancers: identification of an 'inflammatory signature'. J Pathol 202: 265-273, 2004.
21. Shiao YH, Palli D, Caporaso NE, Alvord WG, Amorosi A, Nesi G, Saieva C, Masala G, Fraumeni JF Jr and Rice JM: Genetic and immunohistochemical analyses of p53 independently predict regional metastasis of gastric cancers. Cancer Epidemiol Biomarkers Prev 9: 631-633, 2000.
22. McDonald JW and Pilgram TK: Nuclear expression of p53, p21 and cyclin D1 is increased in bronchioloalveolar carcinoma. Histopathology 34: 439-446, 1999.
23. Yamaguchi T, Kakefuda R, Tanimoto A, Watanabe Y and Tajima N: Suppressive effect of an orally active MEK1/2 inhibitor in two different animal models for rheumatoid arthritis: a comparison with leflunomide. Inflamm Res 61: 445-454, 2012.
24. Yamaguchi T, Kakefuda R, Tajima N, Sowa Y and Sakai T: Antitumor activities of JTP-74057 (GSK1120212), a novel MEK1/2 inhibitor, on colorectal cancer cell lines *in vitro* and *in vivo*. Int J Oncol 39: 23-31, 2011.
25. Cappella P, Gasparri F, Pulici M and Moll J: Cell proliferation method: Click chemistry based on BrdU coupling for multiplex antibody staining. Curr Protoc Cytom 72: 7 34 31-17, 2015.
26. Gartel AL and Radhakrishnan SK: Lost in transcription: p21 repression, mechanisms, and consequences. Cancer Res 65: 3980-3985, 2005.
27. Deng C, Zhang P, Harper JW, Elledge SJ and Leder P: Mice lacking p21CIP1/WAF1 undergo normal development, but are defective in G1 checkpoint control. Cell 82: 675-684, 1995.
28. Dulic V, Kaufmann WK, Wilson SJ, Tlsty TD, Lees E, Harper JW, Elledge SJ and Reed SI: p53-dependent inhibition of cyclin-dependent kinase activities in human fibroblasts during radiation-induced G1 arrest. Cell 76: 1013-1023, 1994.
29. Meloche S and Pouyssegur J: The ERK1/2 mitogen-activated protein kinase pathway as a master regulator of the G1- to S-phase transition. Oncogene 26: 3227-3239, 2007.
30. Chambard JC, Lefloch R, Pouyssegur J and Lenormand P: ERK implication in cell cycle regulation. Biochim Biophys Acta 1773: 1299-1310, 2007.
31. Yao G, Lee TJ, Mori S, Nevins JR and You L: A bistable Rb-E2F switch underlies the restriction point. Nat Cell Biol 10: 476-482, 2008.
32. Waxman S and Anderson KC: History of the development of arsenic derivatives in cancer therapy. Oncologist 6 (Suppl 2): S3-S10, 2001.
33. Fu WJ, Li BL, Wang SB, Chen ML, Deng RT, Ye CQ, Liu L, Fang AJ, Xiong SL, Wen S, *et al*: Changes of the tubular markers in type 2 diabetes mellitus with glomerular hyperfiltration. Diabetes Res Clin Pract 95: 105-109, 2012.
34. Fuster D, Torregrosa JV, Setoain X, Doménech B, Campistol JM, Rubello D and Pons F: Localising imaging in secondary hyperparathyroidism. Minerva Endocrinol 33: 203-212, 2008.
35. Nigg EA: Cyclin-dependent protein kinases: Key regulators of the eukaryotic cell cycle. Bioessays 17: 471-480, 1995.
36. Lavi O, Ginsberg D and Louzoun Y: Regulation of modular Cyclin and CDK feedback loops by an E2F transcription oscillator in the mammalian cell cycle. Math Biosci Eng 8: 445-461, 2011.
37. Arellano M and Moreno S: Regulation of CDK/cyclin complexes during the cell cycle. Int J Biochem Cell Biol 29: 559-573, 1997.
38. Hiyama H, Iavarone A and Reeves SA: Regulation of the cdk inhibitor p21 gene during cell cycle progression is under the control of the transcription factor E2F. Oncogene 16: 1513-1523, 1998.
39. Orlando DA, Lin CY, Bernard A, Wang JY, Socolar JE, Iversen ES, Hartemink AJ and Haase SB: Global control of cell-cycle transcription by coupled CDK and network oscillators. Nature 453: 944-947, 2008.
40. Davies MA and Samuels Y: Analysis of the genome to personalize therapy for melanoma. Oncogene 29: 5545-5555, 2010.
41. Musilova K and Mraz M: MicroRNAs in B-cell lymphomas: How a complex biology gets more complex. Leukemia 29: 1004-1017, 2015.
42. Vosa U, Vooder T, Kolde R, Fischer K, Välk K, Tõnisson N, Roosipuu R, Vilo J, Metspalu A and Annilo T: Identification of miR-374a as a prognostic marker for survival in patients with early-stage nonsmall cell lung cancer. Genes Chromosomes Cancer 50: 812-822, 2011.
43. Wu H and Mo YY: Targeting miR-205 in breast cancer. Expert Opin Ther Targets 13: 1439-1448, 2009.
44. Gregory PA, Bert AG, Paterson EL, Barry SC, Tsykin A, Farshid G, Vadas MA, Khew-Goodall Y and Goodall GJ: The miR-200 family and miR-205 regulate epithelial to mesenchymal transition by targeting ZEB1 and SIP1. Nat Cell Biol 10: 593-601, 2008.